# Influence of the Degree of Calcination of Eggshell on the Strength, Hydration, and Microstructure of Cementitious Mortars

*Sohail Maqsood [1,*], Safi Ur Rehman [2], Muhammad Afzal [2]*

*[1,*] Independent researcher, formerly associated with the Department of Civil and Environmental Engineering, Khalifa University of Science and Technology, Abu Dhabi, UAE. (engr.sohailbhatti@hotmail.com)*
*[2] Department of Civil and Environmental Engineering, Khalifa University of Science and Technology, Abu Dhabi, UAE.*
*[3]Department of Civil and Environmental Engineering (IBM), The Norwegian University of Science and Technology (NTNU), Trondheim 7491, Norway*

***Abstract:*** *Waste eggshell is a biological limestone with the potential to partially replace Portland cement in cementitious mixes, in both calcined and uncalcined states. However, the performance of Calcined Eggshells (CES) is strongly influenced by thermal treatment, as it removes the organic membrane and may alter the calcite-rich phase. This study aims to investigate the influence of calcination temperature and holding duration on the fresh behaviour, 28-day compressive strength, hydration, and microstructure of cementitious mixes containing eggshells as a partial cement replacement. Eggshells were calcined at 400, 600, and 800 °C for 1, 2, and 3 h and replaced with cement at the replacement levels of 5%, 10%, and 15%. The experimental program consisted of two sequential stages, where the first stage aimed to select representative mixtures for detailed hydration and microstructural analysis in the second stage. In the first stage, flow consistency and 28-day compressive strength were measured for all mixes containing CES, and compared with the control mix, mixes with industrial-grade extra pure limestone (LS), and mixes with uncalcined eggshells (ES). Based on phase assemblage, mixtures were classified into calcite-rich (undecomposed) and partially decomposed calcination regimes. Flow consistency and 28-day compressive strength testing identified CES calcined at 600 °C for 2 h at 5% replacement (CES5(600-2)) as the best-performing calcite-rich mixture, and CES calcined at 800 °C for 3 h at 15% replacement (CES15(800-3)) as the best-performing partially decomposed mixture. Thermogravimetric analysis (TGA) showed that CES5(600-2) achieved the highest bound-water content (25.13%) among calcite-rich mixtures, indicating enhanced hydration, while CES15(800-3) exhibited a markedly elevated calcium hydroxide content (21.21%) attributable to the combined contribution of cement hydration and hydration of residual CaO from calcination. Scanning electron microscopy corroborated these findings, revealing a well-developed C-S-H-rich matrix in CES5(600-2) and a highly complex heterogeneous microstructure in CES15(800-3). The results demonstrate that the degree of calcination governs the phase assemblage and hydration pathway of CES, offering guidance for optimising eggshell-derived materials as sustainable supplementary cementitious materials.*

***Keywords:*** *Calcined eggshells; calcite; compressive strength; thermogravimetric analysis; bound water; calcium hydroxide*

## 1. Introduction

Limestone (LS) can be used up to 10% replacement without sacrificing the compressive strength [1]. As a partial replacement for cement, LS fillers can improve hydration in a low water-to-cement ratio [2]. Eggshell (ES) is a biological limestone that contains 94% - 95% Calcite [3,4], and can be used in place of LS in calcium silicate products [5,6]. LS is completely reactive up to 5% replacement [7], while some studies also recommend 5% ES replacement for the optimal strength gain with OPC [8–16]. Moreover, incorporating ES also reduces setting time [17,18], improves radiation shielding properties [19,20], enhances thermal properties [21], and can be used up to a 20 % replacement level under elevated temperature conditions [22]. In general, using eggshells either in an uncalcined or calcined state has a positive impact on the hydration of cementitious materials [18,23–25].

Although cracking and grinding the shell can remove part of the organic membrane [26], the complete removal of residual organic matrix is not convenient and practical. The presence of the organic part results in reduced compressive strength when used as a cement replacement in cementitious products [3,8,22,27]. Importantly, the chemical interaction between $Ca^{2+}$ and the ES surface is relatively weaker than that of LS due to the presence of the organic membrane, resulting in less dense heterogeneous nucleation and lower hydration [28]. Regarding limitations associated with rheology, the presence of an organic matrix in eggshells potentially results in hindrance in pumping, spreading, and compacting due to higher static yield stress in cement paste [29]. Therefore, removing the organic membrane results in the purer form of limestone and with enhanced properties for application as a cement replacement. It can typically be done by either heat treatment like calcination [30], or a chemical treatment like a reaction with bleach solution [31]. The former method is recommended for its effectiveness [30].

Many studies have been reported on the use of Calcined Eggshells (CES) as a cement replacement obtained through different calcination conditions. Cree and Pliya [22] report 450 °C, and Wei et al. [29] recommend 500 °C to completely

remove the organic matrix for cement-based materials. Ngayakamo et al. [32] used eggshells calcined at 800 ºC for 1.5 hours with optimal replacement of 10% for improved microstructure and hydration. CES improves both short-term and long-term strength, reduces total porosity, while CaO turns into amorphous Calcium Hydroxide (CH), causing filling of pores [27]. However, the presence of CaO is possible only when calcination is performed at higher temperatures. For instance, calcination at 900 ºC for two hours completely decomposes $CaCO^3$ into CaO [31].

Given the relatively better performance of calcined eggshell powder (CES), several studies have investigated the influence of calcination conditions, particularly temperature and holding duration, on its behaviour as a cementitious material. These processing parameters determine the degree of calcination by controlling the extent of thermal decomposition of calcium carbonate ($CaCO_3$), thereby governing the proportions of residual calcite and dissociated lime (CaO and its hydration product, $Ca(OH)_2$). Şenol and Çalışkan [16] investigated CES calcined at 800°C and 900°C for a fixed holding duration of 2 h with cement replacement levels ranging from 5% to 15% and reported that eggshells calcined at 900°C exhibited superior mechanical performance at a 5% replacement level. Wang et al. [27] employed thermogravimetric analysis to investigate the hydration behaviour of ternary OPC–GGBS–CES blends containing eggshells calcined at 900°C for holding durations of 10, 20, and 30 min. Their study demonstrated that the balance between residual $CaCO_3$ and newly formed CaO influenced hydration and compressive strength; however, the contribution of CES remained difficult to isolate because of the simultaneous incorporation of GGBS. In a related study, Maqsood and Eddie [18] investigated eggshells calcined at 400°C, 600°C, and 800°C for temperature holding durations of one, two, and three hours. Nevertheless, their investigation was limited to early-age properties, including setting time and heat of hydration. Collectively, these studies demonstrate that calcination conditions substantially influence the performance of CES; however, the relationship between the degree of calcination, phase evolution, hydration behaviour, and mechanical performance remains insufficiently understood.

Hydration is a fundamental process governing the development of the cementitious matrix and, consequently, its mechanical performance. In calcium-silicate-based cement systems, hydration produces C-S-H and CH together with secondary AFt and AFm phases; in calcium-carbonate-containing systems, carbonate can additionally participate in the formation of calcium carboaluminate phases [33–36]. Although compressive strength provides an indirect indication of hydration development, thermogravimetric analysis (TGA) provides a quantitative means of assessing hydration-related mass losses through the determination of chemically bound water and CH contents [34–41]. Previous studies have used TGA to distinguish dehydration, dehydroxylation, and decarbonation regions and to evaluate hydration in cementitious systems with limestone and SCMs [37–39,41,42].

Calcium-carbonate-bearing particles can influence hydration not only through physical filler effects but also by providing surfaces for heterogeneous nucleation of hydration products. The extent of this effect can depend on particle size, surface characteristics, and the amount of carbonate-containing material [43–50]. Similar nucleation effects have been reported for eggshell-derived calcium carbonate, indicating that eggshell particles can provide additional surfaces for hydration-product formation [51]. Consequently, the effect of calcination on eggshell hydration may arise from the combined influence of organic-matrix removal, changes in particle characteristics, and progressive transformation of $CaCO_3$ into dissociated lime. However, the transition from predominantly calcite-rich eggshell powder to partially decomposed systems containing residual calcite together with dissociated lime has received limited systematic investigation within a common cementitious system. Previous hydration studies have considered eggshells and calcined eggshells, but the influence of intermediate calcination states on later-age hydration and mechanical performance remains insufficiently resolved [18,51].

Accordingly, this study establishes the relationship between the degree of calcination of eggshell powder, the resulting phase assemblage, and the hydration, microstructural evolution, and mechanical performance of cementitious systems. Calcination temperature and holding duration are treated as processing variables used to generate different degrees of calcination. Eggshell powders produced under different calcination conditions were initially evaluated through flow consistency and compressive strength testing to identify representative mixtures from the calcite-rich and partially decomposed calcination regimes. Detailed hydration and microstructural characterization were subsequently carried out using Thermogravimetric Analysis (TGA) and Scanning Electron Microscopy (SEM) to elucidate the mechanisms governing the observed performance. The findings provide new insight into the role of the degree of calcination in controlling the reactivity of calcined eggshell powder and contribute to the development of sustainable cementitious materials through the effective valorisation of waste eggshells.

## 2. Materials and Methods

### *2.1. Materials*

The binder used in this study was CEM I 52.5 N conforming to the specifications of BS EN 197-1 [52]. Eggshells were collected from different restaurants, cleaned with water, air-dried, and then ground in a ball mill under a constant weight of 12 kg for the duration of 6 hours.

To get the CES, ground eggshells were calcined in an electric furnace at 400ºC, 600ºC and 800ºC for the temperature holding duration of one, two, and three hours. In this way, nine different types of calcined eggshells were obtained, as shown in Table 1 below. Both ES and CES were sieved through an ASTM No. 200 sieve before incorporation in mixes.

Industrial-grade extra pure limestone (LS) was also used to compare the results associated with ES and CES. Simple tap water was used for the preparation of mixes, while CEN standard sand, as explained in BS EN 196-1, was used for mortar specimens [53].

Table 1: Details of calcined eggshells

| Designation | Description | Colour | Photo |
|---|---|---|---|
| CES-400(1) | Eggshells calcined at 400ºC for one hour | Light beige or off-white |  |
| CES-400(2) | Eggshells calcined at 400ºC for two hours | |  |
| CES-400(3) | Eggshells calcined at 400ºC for three hours | | 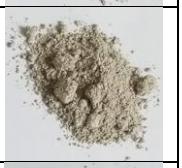 |
| CES-600(1) | Eggshells calcined at 600ºC for one hour | Darker grey or gunmetal |  |
| CES-600(2) | Eggshells calcined at 600ºC for two hours | |  |
| CES-600(3) | Eggshells calcined at 600ºC for three hours | |  |
| CES-800(1) | Eggshells calcined at 800ºC for one hour | Silver-grey or ash grey |  |
| CES-800(2) | Eggshells calcined at 800ºC for two hours | |  |
| CES-800(3) | Eggshells calcined at 800ºC for three hours | | 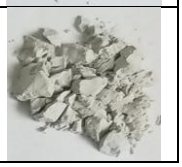 |

### *2.2. Materials Properties and Characterisation*

The chemical compositions of OPC, limestone (LS), eggshell powder (ES), and the calcined eggshell powders (CES) were determined using X-ray fluorescence (XRF) analysis. The corresponding oxide compositions are summarized in

Table 2. Based on the oxide composition, the Bogue phase composition of OPC was calculated, consisting of 62.89% $C_3S$, 9.06% $C_2S$, 9.73% $C_3A$, and 9.52% $C_4AF$. These values indicate that the cement was predominantly composed of alite ($C_3S$), which is characteristic of CEM I 52.5 N cement.

Table 2: Oxide compositions of OPC, ES, LS, and CES

| Component | OPC | LS | ES | CES400(1) | CES400(2) | CES400(3) | CES600(1) | CES600(2) | CES600(3) | CES800(1) | CES800(2) | CES800(3) |
|---|---|---|---|---|---|---|---|---|---|---|---|---|
| | % | % | % | % | % | % | % | % | % | % | % | % |
| MgO | 0.96 | 0.55 | 1.08 | 1.06 | 0.87 | 1.16 | 1.07 | 0.82 | 1.02 | 1.22 | 1.20 | 1.12 |
| $Al_2O_3$ | 5.67 | 0.10 | 0.10 | 0.08 | 0.14 | 0.13 | 0.13 | 0.10 | 0.22 | 0.11 | 0.11 | 0.10 |
| $SiO_2$ | 19.70 | 1.10 | 1.42 | 1.46 | 1.26 | 1.29 | 1.49 | 1.27 | 2.21 | 1.28 | 1.15 | 1.28 |
| $P_2O_5$ | 0.14 | 0.10 | 0.50 | 0.49 | 0.46 | 0.48 | 0.50 | 0.49 | 0.48 | 0.48 | 0.52 | 0.52 |
| $SO_3$ | 3.86 | 0.03 | 0.83 | 0.44 | 0.47 | 0.49 | 0.40 | 0.41 | 0.56 | 0.55 | 0.55 | 0.55 |
| $K_2O$ | 0.71 | 0.06 | 0.16 | 0.16 | 0.16 | 0.15 | 0.16 | 0.16 | 0.19 | 0.15 | 0.14 | 0.16 |
| CaO | 65.40 | 97.90 | 95.80 | 96.20 | 96.50 | 95.90 | 96.10 | 96.60 | 95.20 | 95.70 | 95.90 | 96.20 |
| $Fe_2O_3$ | 3.13 | 0.04 | 0.06 | 0.05 | 0.06 | 0.05 | 0.05 | 0.06 | 0.06 | 0.04 | 0.04 | 0.04 |
| Others | 0.43 | 0.11 | 0.04 | 0.07 | 0.08 | 0.35 | 0.11 | 0.10 | 0.07 | 0.48 | 0.39 | 0.03 |

The physical characteristics of the powders were evaluated by determining their specific surface area and particle size distribution. The specific surface area was measured using the Brunauer–Emmett–Teller (BET) method, while the particle size distribution (PSD) was determined by laser diffraction using ethanol as the dispersing medium. The PSD curves are presented in Figure 1, whereas the BET specific surface areas and characteristic particle sizes, including D[4,3], D(50), and D(90), are summarized in Table 3.

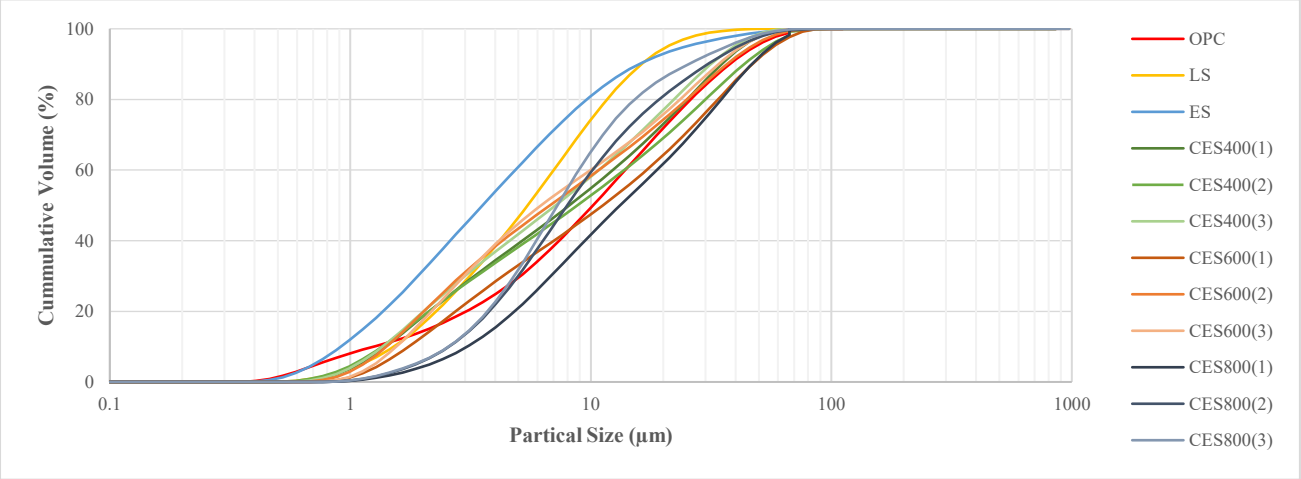


Figure 1: Particle size distribution of OPC, limestone, eggshells and calcined eggshells

Table 3: Details of D[4,3], D(50), and D(90) particle sizes of OPC, LS, ES, and CES

| Material | BET Surface Area | D[4,3] | D(50) | D(90) |
|---|---|---|---|---|
| | $m^2/kg$ | µm | µm | µm |
| OPC | 1.40 | 17.530 | 11.564 | 42.865 |
| LS | 1.53 | 8.544 | 6.202 | 18.468 |
| ES | 1.91 | 7.801 | 4.032 | 18.077 |
| CES-400(1) | 5.38 | 15.555 | 9.245 | 39.748 |

| | | | | |
|---|---|---|---|---|
| CES-400(2) | 5.41 | 18.550 | 9.966 | 49.270 |
| CES-400(3) | 5.44 | 13.980 | 8.114 | 35.872 |
| CES-600(1) | 1.87 | 21.016 | 12.763 | 53.368 |
| CES-600(2) | 2.22 | 15.532 | 7.687 | 41.876 |
| CES-600(3) | 2.44 | 14.428 | 7.059 | 38.641 |
| CES-800(1) | 2.11 | 22.512 | 15.035 | 53.139 |
| CES-800(2) | 2.80 | 14.385 | 9.067 | 34.856 |
| CES-800(3) | 3.44 | 60.945 | 15.551 | 67.225 |

Thermogravimetric analysis (TGA) was performed to investigate the thermal decomposition behaviour of ES and LS and to determine their calcium carbonate contents. Based on the TGA results, the raw ES contained approximately 96.58 wt.% calcium carbonate (calcite), whereas the remaining fraction mainly consisted of volatile and organic constituents. In contrast, LS contained approximately 99.62 wt.% calcium carbonate, indicating negligible amounts of volatile and organic matter. A representative TGA thermogram of ES is presented in Figure 2.

The mineralogical compositions of ES and CES were characterized using X-ray diffraction (XRD), and quantitative phase analysis was performed by the Rietveld refinement method. The XRD patterns of ES and CES, together with that of limestone (LS), are presented in Figure 3 for comparison. The crystalline phases identified in the calcined eggshell powders included calcite ($CaCO_3$), calcium hydroxide (CH), and calcium oxide (CaO). Since CaO readily reacts with atmospheric moisture to form CH during sample handling and storage [54–56], accurately distinguishing between these two phases may introduce uncertainty. Therefore, the combined amount of CaO and CH is also referred to as dissociated lime throughout this study.

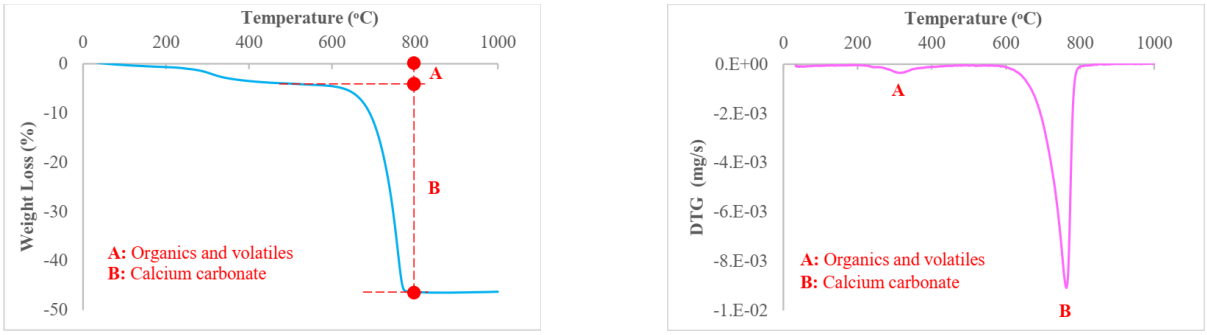


(a) (b)

Figure 2: Typical thermogram for eggshell (a) weight loss associated with volatile/organic and mineral part [3], (b) Differential Thermogravimetric Curve (DTG). Adapted from [3].

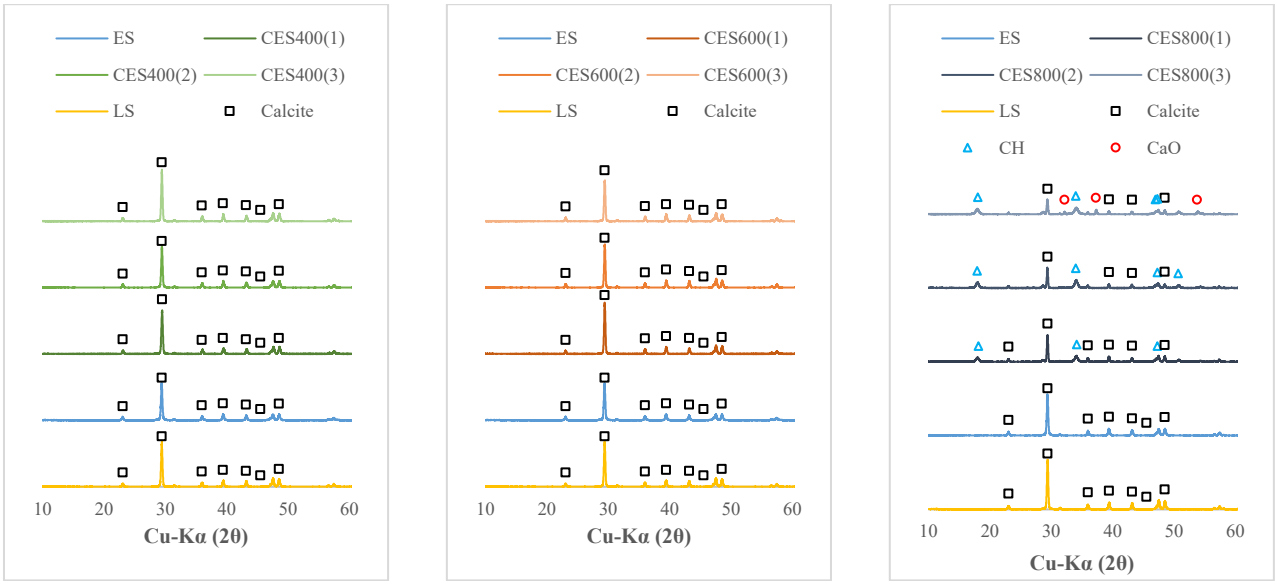


(a) (b) (c)

Figure 3: XRD spectrum indicating the presence of calcite, CaO and CH: (a) eggshells calcined at 400°C, (b) eggshells calcined at 600°C and (c) eggshells calcined at 800°C

The Rietveld refinement indicated that CES800(1) consisted of 63% calcite and 37% CH, whereas CES800(2) contained 48% calcite and 52% CH. CES800(3) comprised 38% calcite, 55% CH, and 7% CaO. These quantitative phase assemblages were subsequently used to determine the degree of calcination of the CES samples.

### *2.3. Mix Proportion*

Two types of cementitious mixtures, namely mortar and cement paste, were prepared to evaluate the influence of the calcination state of eggshell powder on the performance and hydration of cementitious materials.

Mortar mixtures were prepared for the determination of flow consistency, compressive strength, and pore structure through Mercury Intrusion Porosimetry (MIP). All mortar mixtures were proportioned in accordance with BS EN 196-1, maintaining a binder-to-sand ratio of 1:3 and a constant water-to-binder ratio of 0.50. Ordinary Portland cement (OPC) was partially replaced by limestone (LS), eggshell powder (ES), and the nine calcined eggshell powders (CES) at replacement levels of 5%, 10%, and 15% by mass of cement. A control mixture containing only OPC was also prepared. The detailed mortar mix proportions are presented in Table 4.

Table 4: Mix Proportion for mortar specimens as per BS EN 196-1

| Mix | OPC (g) | Replacement (g) | Fine Aggregates (g) | W/B | A/B |
|---|---|---|---|---|---|
| Control | 900 | - | 2700 | 0.5 | 3 |
| 5% Replacement | 855 | 45 | 2700 | 0.5 | 3 |
| 10% Replacement | 810 | 90 | 2700 | 0.5 | 3 |
| 15% Replacement | 765 | 135 | 2700 | 0.5 | 3 |

Cement paste specimens were prepared for thermogravimetric analysis (TGA) to investigate the hydration characteristics of the selected mixtures. A constant water-to-binder ratio of 0.30, corresponding to the standard consistency of the OPC used in this study, was adopted for all paste mixtures. The paste mixtures contained the same binder compositions as the corresponding mortar mixtures but without the addition of fine aggregate.

The mixtures were designated as M-XR(T-H), where M denotes mix, X represents the replacement material (LS, ES, or CES), R is the cement replacement level (%), T is the calcination temperature (°C), and H is the temperature holding duration (h). For example, M-CES5(400-2) denotes a mix containing calcined eggshell powder (CES) prepared by calcination at 400°C for 2 h and incorporated as a 5% replacement of cement.

### *2.4. Test Methods*

#### *2.4.1. Flow Consistency*

The consistency of fresh mortar was determined immediately after mixing in accordance with BS EN 1015-3. The measured flow values were used to evaluate the influence of calcination temperature and replacement level on the workability of the mortar mixtures.

#### *2.4.2. Compressive Strength*

Mortar specimens having dimensions of 40 × 40 × 40 mm were prepared following BS EN 196-1. After casting, the specimens were covered to prevent moisture loss and demoulded after 24 h. The specimens were subsequently cured in lime-saturated water at 20 ± 2 °C until the designated testing ages.

Compressive strength tests were conducted at 28 days using a universal testing machine. The reported values represent the average compressive strength obtained from three specimens for each mixture.

#### *2.4.3. Thermogravimetric Analysis*

Thermogravimetric analysis (TGA) was carried out to evaluate the hydration behaviour of the selected cement pastes. The paste specimens were prepared using a water-to-binder ratio of 0.30 and cured for 28 days. Hydration was terminated prior to testing using solvent exchange with ethanol.

The dried samples were ground to pass a 75 μm sieve before testing. Samples were put into 20mg alumina crucible, and $Al_2O_3$ powder was used as reference material. Each sample was heated from ambient temperature to 1000°C at a heating rate of 10°C/min under an argon atmosphere.

The derivative thermogravimetric (DTG) curves were used to identify the decomposition regions associated with hydration products. The contents of calcium hydroxide and chemically bound water were determined from the corresponding mass losses using the tangent method to calculate the degree of hydration.

#### *2.4.4. Scanning Electron Microscopy*

The morphology and microstructure of the hydrated cement matrix were examined using Scanning Electron Microscopy (SEM). Twenty-eight-day-old mortar specimens were selected for analysis. Small fragments were collected from the interior of the specimens to avoid surface contamination and immediately immersed in ethanol to terminate cement hydration through the solvent exchange method. The specimens were subsequently dried in an oven at 60 °C for 24 h and coated with a thin layer of gold by sputter coating to improve electrical conductivity during imaging.

SEM observations were performed using secondary electron (SE) imaging at an accelerating voltage of 20 kV and a magnification of 10,000x.

### *2.5. Experimental Program*

The experimental programme consisted of two sequential stages, as illustrated in Figure 4.

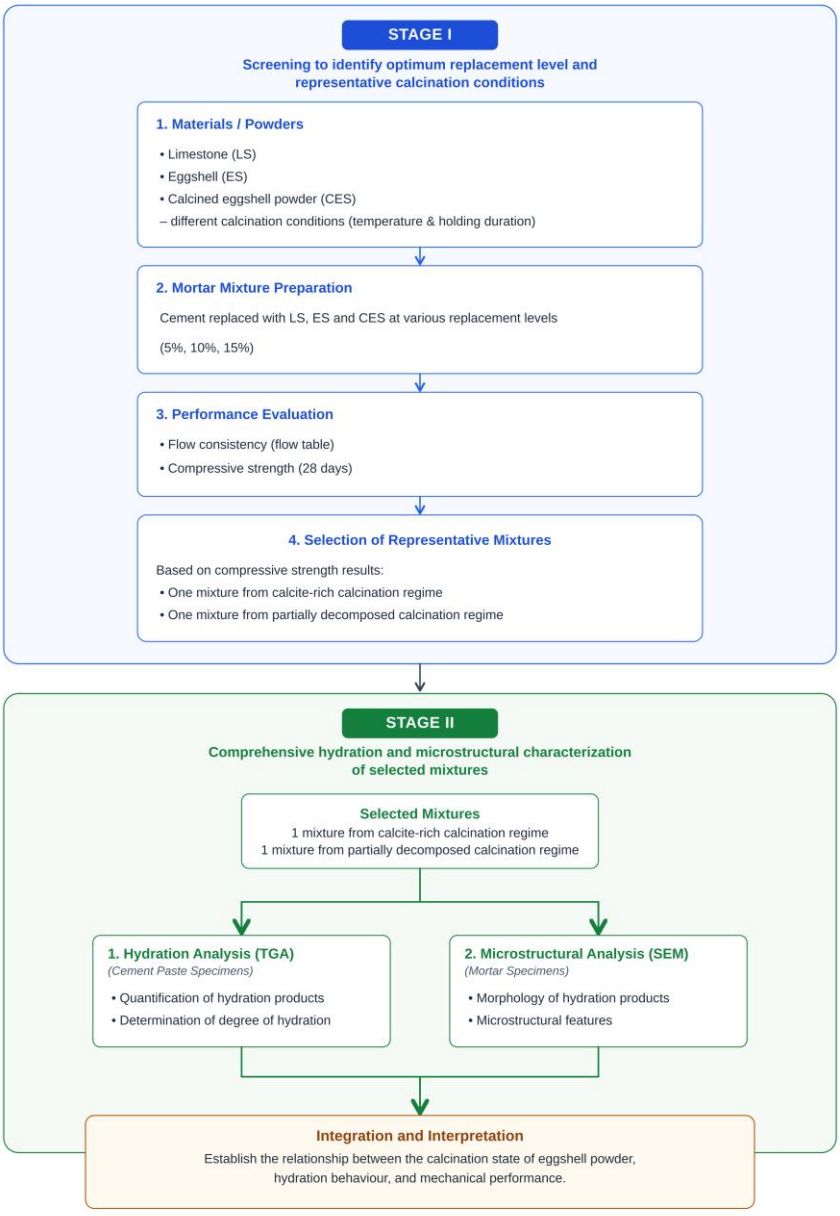


Figure 4: Scope of experimental work

In Stage I, mortar mixtures containing LS, ES, and CES were prepared to identify the optimum replacement level and representative calcination conditions through flow consistency and compressive strength testing. Based on the mechanical performance, one representative mixture from the calcite-rich calcination regime and one representative mixture from the partially decomposed calcination regime were selected for detailed investigation.

In Stage II, the selected mixtures were subjected to comprehensive hydration and microstructural characterization. TGA was performed on cement paste specimens to quantify hydration products and chemically bound water, whereas scanning electron microscopy (SEM) was conducted on mortar specimens to examine the morphology and microstructural development of the hydrated matrix. The combined results were used to relate the calcination state of eggshell powder to hydration behaviour and mechanical performance.

## 3. Results and Discussions

### *3.1. Flow Consistency*

Figure 5 below depicts the flow consistency of mortar mixes containing LS, ES, and CES at different replacement levels, compared to the control mix with consistency of 169mm. Both ES and LS produced a replacement-dependent response, while LS depicted a good flowability response ranging from 180 mm at 5% replacement to 214 mm at 15% replacement. This is justified by the previous studies, which report that LS can improve fluidity or reduce the water demand required to achieve a given flowability [57–60]. The lower flowability of mixes containing ES is due to the presence of organic members, which results in difficulty in spreading [29].

The CES-based mixes showed variation compared to ES-based mixes in the flow consistency, which depicts the change in the rheological behavior due to combined changes in physical and chemical characteristics of eggshells induced by thermal treatment. Unlike mixes containing LS and ES, CES-based mixes exhibited a non-monotonic variation in flow consistency with calcination conditions and replacement level. Overall, thermal treatment slightly improves the rheology and eliminates the limitations associated with the presence of organic matrix. Thermal treatment removes the organic matrix, modifies the surface characteristics, particle packing, and ultimately the quantity of water available to flow [16].

In summary, LS incorporation improved the workability of the mortar mixtures, whereas the presence of the organic membrane reduced the flowability of ES-based mixtures. Calcination altered and improved the flow behavior of eggshell powder, resulting in a more variable rheological response.

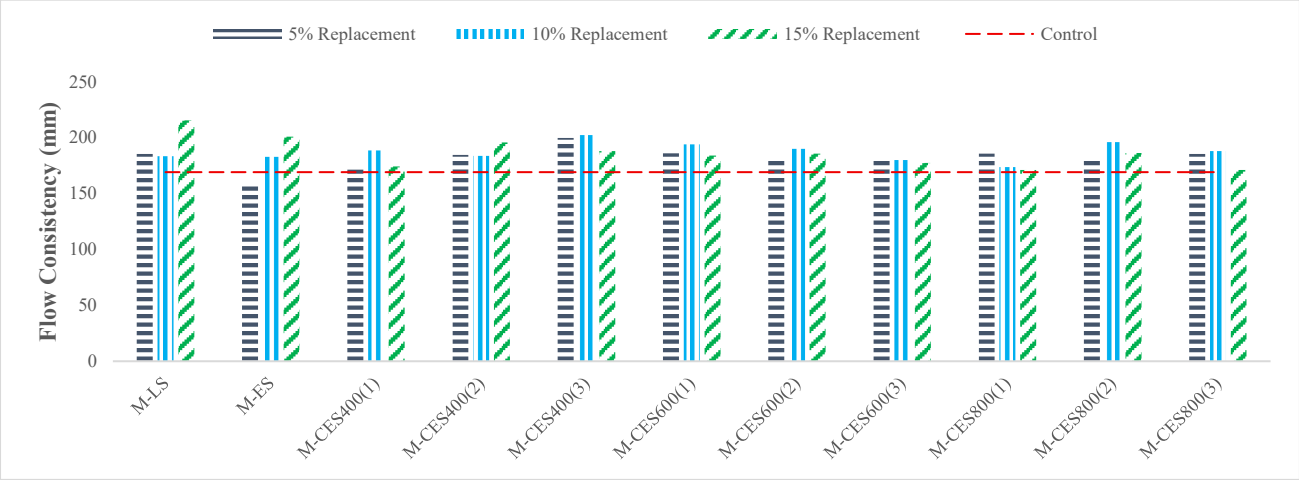


Figure 5: Flow consistency of mixes with LS, ES, and CES compared with the control mix

### *3.2. Compressive Strength*

#### *3.2.1. Effect of Replacement Level and Calcination Regime*

For comparison, excluding the control mixture, the mixtures were broadly divided into two categories according to the degree of calcination: calcite-rich (predominantly undecomposed) mixtures and partially decomposed mixtures. The former comprises limestone, uncalcined eggshells, and eggshells calcined at temperatures below 800 °C, whereas the latter comprises eggshells calcined at temperatures above 800 °C. As shown in Figure 6, the limestone-containing mixtures exhibited higher compressive strength than the uncalcined eggshell mixtures, which can be attributed to the higher purity of limestone and the absence of the organic membrane present in eggshells [8]. Similarly, the calcined eggshell mixtures generally exhibited higher compressive strength than the uncalcined eggshell mixtures, indicating the

beneficial effect of thermal treatment and removal of the organic matrix. For the calcite-rich mixtures, the highest compressive strength was generally obtained at a 5% replacement level. In contrast, the strength response of the partially decomposed mixtures was less systematic with replacement level, which may be associated with the more complex phase assemblage resulting from the partial decomposition of $CaCO_3$ and the formation of CaO and its subsequent hydration product, $Ca(OH)_2$.

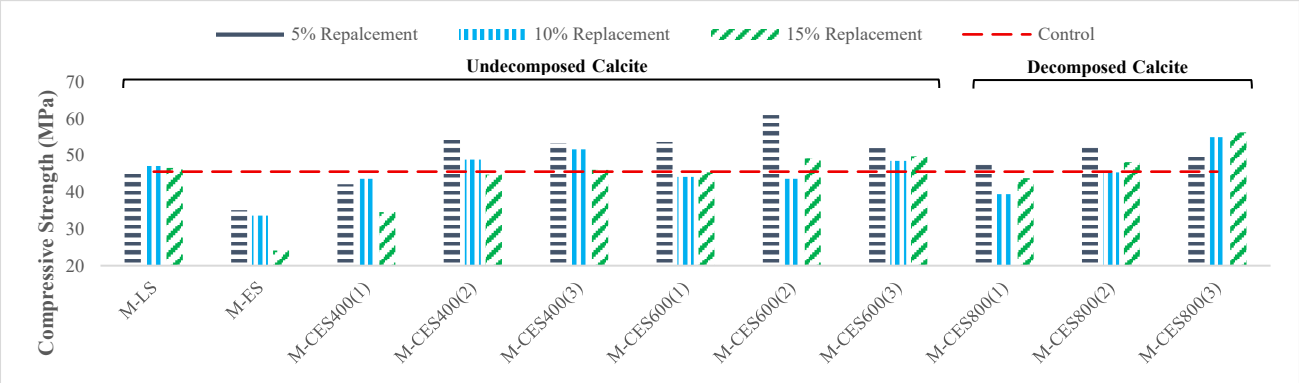


Figure 6: 28th day compressive strength of mortar specimens containing LS, ES and CES at different replacement, temperature and temperature holding duration in comparison with the control mix

### *3.2.2. Effect of Calcination Temperature and Holding Duration*

In addition, the effect of temperature holding duration on compressive strength is presented in Figure 7. For the calcite-rich mixtures, the highest compressive strength was generally obtained after a 2 h holding duration, as shown in Figure 7(a). In contrast, the mixtures containing CES calcined at 800 °C exhibited their highest strength after a 3 h holding duration. This difference indicates that the optimum holding duration may depend on the degree of calcination and the resulting phase assemblage of the eggshell powder. Although a broader range of calcination temperatures would be required to establish the optimum condition for the partially decomposed regime, the present results indicate that CES calcined at 800 °C for 3 h at a 15% replacement level was the highest-performing mixture within the investigated partially decomposed regime. Figure 7(b) further compares the highest-performing mixtures obtained at their respective optimum holding durations for the calcite-rich and partially decomposed regimes.

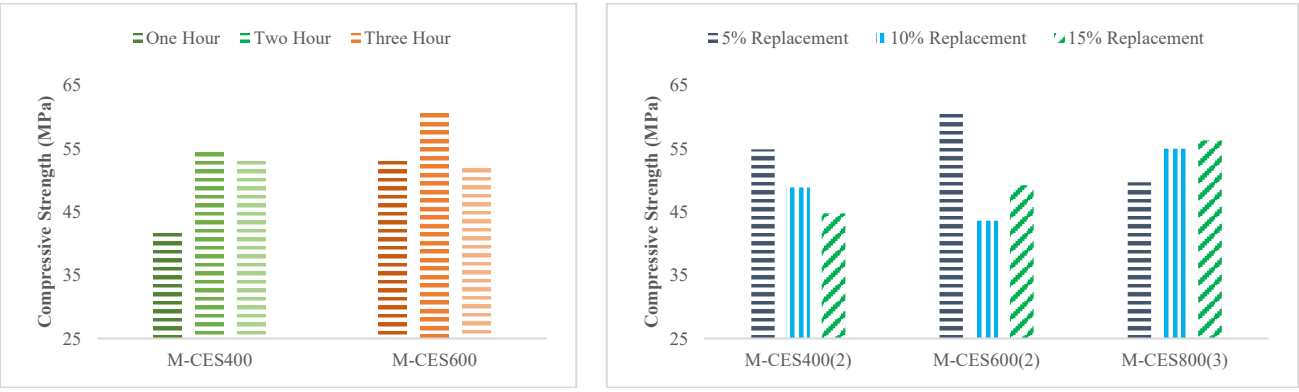


(a) (b)

Figure 7: 28th day compressive strength, (a) Comparison of temperature holding duration for mixes with undecomposed calcined eggshells, (b) Comparison of mixes with optimal temperature holding duration of all three temperatures

### *3.2.3. Filler Effect and Heterogenous Nucleation*

The strength development of calcium-carbonate-containing mixtures can be influenced by both physical filler effects and the ability of carbonate-bearing particles to provide surfaces for heterogeneous nucleation of hydration products. Fine calcium carbonate particles can improve particle packing by occupying voids between cement particles and modifying the particle-size distribution, potentially contributing to a denser cementitious matrix [43,61,62]. In the present study, the D[4,3] particle sizes of LS and ES were approximately 8.54 µm and 7.80 µm, respectively, compared with 17.53 µm for

OPC. Thus, both LS and ES were substantially finer than OPC and could potentially contribute to particle packing and filler effects. Nevertheless, the higher strength of LS-containing mixtures compared with ES-containing mixtures indicates that particle fineness alone cannot explain the observed strength development.

For CES in the calcite-rich regime, the D[4,3] particle size ranged from approximately 15 to 22 μm, which was broadly comparable to that of OPC. Consequently, the conventional particle-packing contribution associated with the introduction of substantially finer particles may be less pronounced for these CES mixtures. The strength development of CES may therefore involve additional mechanisms, including the surface-mediated nucleation of hydration products. The absence of the organic membrane following thermal treatment may further facilitate interaction between the eggshell-derived particles and the cementitious matrix, potentially enhancing heterogeneous nucleation [43]. In contrast, the interpretation of the strength development of CES in the partially decomposed regime is more complex because the phase assemblage includes residual $CaCO_3$ together with CaO and $Ca(OH)_2$ generated during and after calcination. Therefore, the observed strength cannot be attributed solely to a physical filler effect.

### *3.3. Selection of Representative Mixtures*

Based on the compressive-strength results presented in Section 3.2, the mixtures selected for detailed hydration analysis were determined according to their calcination regime and mechanical performance. For the mixtures containing predominantly undecomposed calcite, the 5% replacement level generally provided the highest compressive strength. Accordingly, 5% replacement was selected for investigating the effect of calcination conditions within this regime. CES400-2 and CES600-2 were considered representative calcite-rich conditions, allowing the influence of calcination temperature on hydration to be examined while maintaining the same replacement level and holding duration. For the partially decomposed regime, the replacement-level response was less systematic; therefore, CES15(800-3), which exhibited the highest compressive strength under the investigated 800 °C conditions, was selected as the representative mixture.

The hydration behaviour of the selected CES mixtures was evaluated in comparison with the control mixture, 5% LS, and 5% uncalcined ES. This comparison allows the influence of progressive calcination of eggshell powder on the hydration products and thermal stability of the hydrated cementitious matrix to be examined.

### *3.4. Thermogravimetric Analysis (TGA) and Hydration Mechanism*

#### *3.4.1. Identification of Thermal Decomposition Regions and Hydration Products*

The TG curves for representative mixtures presented in Figure 8-10 can be broadly divided into three principal regions: dehydration ($L_{dh}$), dehydroxylation ($L_{dx}$), and decarbonation ($L_{dc}$). The dehydration region, approximately 50–380 °C, is primarily associated with the removal of chemically and physically bound water from hydration products, including C-S-H, AFt, and AFm phases. The dehydroxylation region between approximately 380 and 550 °C is predominantly associated with the decomposition of calcium hydroxide (CH), whereas the decarbonation region above approximately 550 °C is mainly related to the decomposition of calcium carbonate.

The DTG curves show several characteristic thermal events within these regions. The first two major endothermic peaks, occurring at approximately 85 and 125 °C, can primarily be associated with the dehydration of C-S-H/AFt and AFm phases, respectively. In calcium-carbonate-containing cementitious systems, the AFm phase may include calcium carboaluminate phases formed through the reaction of calcium carbonate with tricalcium aluminate [63]. At 28 days, these phases may occur as a combination of hemicarboaluminate and monocarboaluminate [64,65], although the formation of predominantly monocarboaluminate has also been reported [51].

The third major peak, located at approximately 420 °C, corresponds primarily to the dehydroxylation of CH. The associated mass loss provides an indication of the CH content present in the hydrated system. However, this interpretation requires particular consideration for the CES-containing mixtures. In the case of highly calcined eggshells, particularly CES800, CaO generated during calcination can subsequently react with water to form $Ca(OH)_2$. Therefore, the CH detected by TGA in these mixtures may originate from both cement hydration and hydration of CaO initially present in the calcined eggshell powder. Consequently, a higher CH content does not necessarily indicate a proportionally greater degree of cement hydration.

Two additional thermal events are observed in the decarbonation region. The peak around 600 °C may be associated with the decomposition of metastable calcium carbonate polymorphs, particularly vaterite and aragonite, whereas the peak around 670 °C is primarily associated with calcite decomposition. These carbonate phases may originate from residual or unreacted calcium carbonate in the eggshell powder or from carbonation of the hydrated cementitious matrix [42,66–71]. Therefore, the mass loss in this region should be interpreted as the combined contribution of residual carbonate and carbonation products rather than being attributed exclusively to one source.

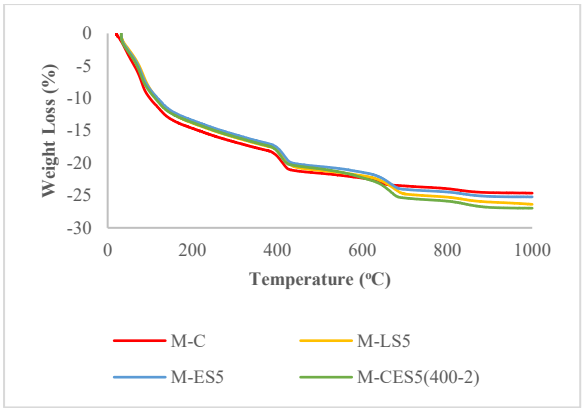


(a)

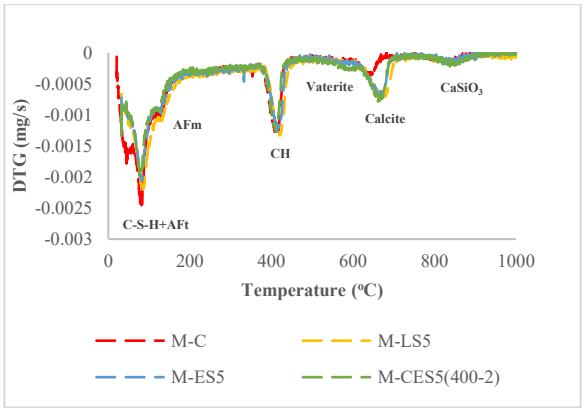


(b)

Figure. 8: TGA for the control specimen with CES400 for two-hour calcination duration at the rate of 5% replacement in comparison with the control specimen containing 100% OPC, specimen with 5% LS, and the specimen with 5% ES (a) weight loss (b) DTG

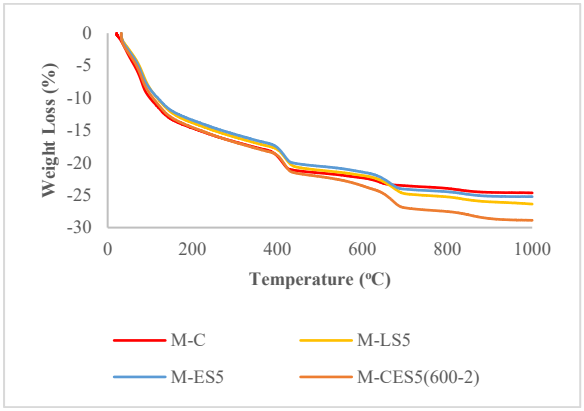


(a)

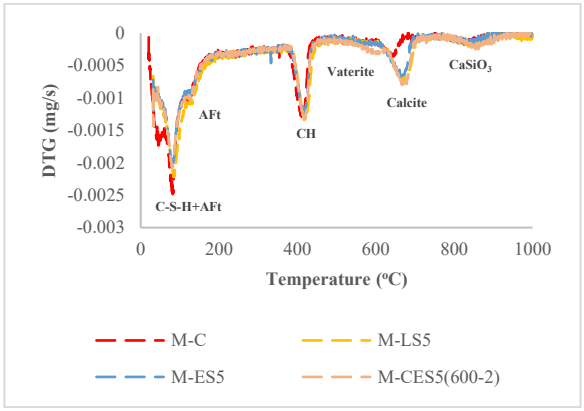


(b)

Figure. 9: TGA for the control specimen with CES600 for two-hour calcination duration at the rate of 5% replacement in comparison with the control specimen containing 100% OPC, specimen with 5% LS, and the specimen with 5% ES (a) weight loss (b) DTG

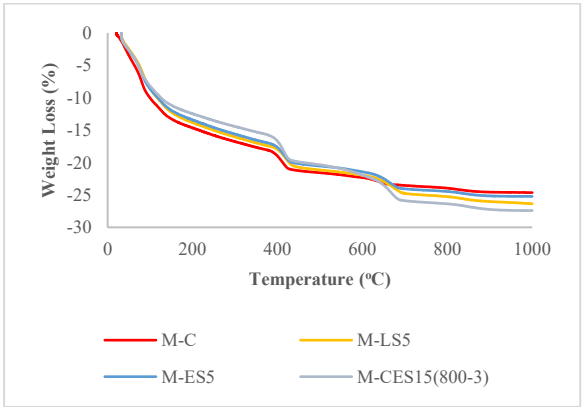


(a)

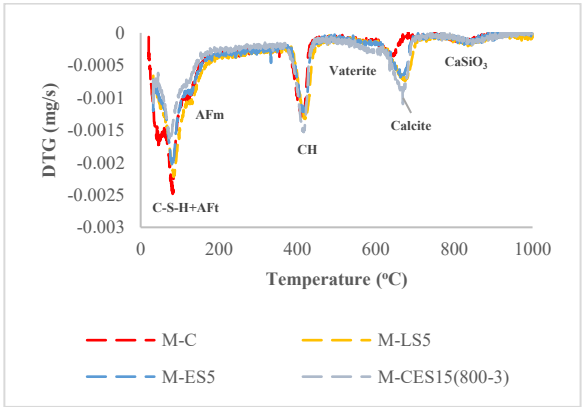


(b)

Figure 10: TGA for the control specimen with CES800 for three-hour calcination duration at the rate of 15% replacement in comparison with the control specimen containing 100% OPC, specimen with 5% LS, and the specimen with 5% ES (a) weight loss (b) DTG

A further thermal event at higher temperature may be associated with calcium metasilicate ($CaSiO_3$), or wollastonite [72–74]. Wollastonite is a calcium silicate mineral containing approximately 48.3% CaO and 51.7% $SiO_2$ and has been investigated as a relatively low-reactivity mineral addition in cementitious systems [75–77]. Nevertheless, the

corresponding mass loss in the present mixtures was only approximately 0.87–1.52%; therefore, its contribution to the overall hydration behaviour is considered negligible.

*3.4.2. Effect of Calcination on Bound Water and Calcium Hydroxide*

The quantitative mass losses obtained from the TG curves and the calculated bound-water and CH contents are presented in Table 5. The results show that the bound-water contents of the LS and CES containing mixtures were generally comparable to or higher than that of the control mixture. The control mixture exhibited a bound-water content of 23.59%, whereas the 5% LS mixture showed a slightly higher value of 24.21%. In contrast, the uncalcined ES mixture exhibited the lowest bound-water content among the reference mixtures, at 22.93%. This lower value is consistent with the comparatively poorer hydration and mechanical performance observed for the uncalcined ES mixture.

The lower bound-water content of ES5 may be associated with the presence of the residual organic membrane, which can interfere with the interaction between the eggshell particles and the cementitious matrix. Following calcination, the bound-water contents generally increased. Among the calcite-rich mixtures, CES600-2 exhibited the highest bound-water content, reaching 25.13%, compared with 23.59% for the control and 24.21% for LS5. This result indicates a greater development of water-bearing hydration products in CES600-2 and is consistent with its superior compressive-strength performance.

The CH contents show a similar but not identical trend. The control, LS5, and ES5 mixtures exhibited CH contents of 15.48%, 16.58%, and 15.86%, respectively. The CES400 and CES600 mixtures generally exhibited somewhat higher CH contents, with CES600-2 reaching 17.68%. The relatively high CH content of CES600-2, together with its highest bound-water content, suggests enhanced hydration within the calcite-rich regime.

However, the interpretation becomes more complex for the partially decomposed mixture. CES15(800-3) exhibited a CH content of 21.21%, substantially higher than that of the control and calcite-rich mixtures. This increase cannot be attributed solely to enhanced cement hydration because calcination at 800 °C promotes partial decomposition of $CaCO_3$ and formation of CaO. The subsequent hydration of this CaO can produce additional $Ca(OH)_2$, which contributes directly to the measured CH content. Consequently, the CH value obtained for CES15(800-3) represents the combined contribution of cement hydration and hydration of CaO originating from the calcined eggshell.

Table 5: Weight loss during TGA, bound water and calcium hydroxide content for all mixes

| Specimen | Dehydration ($L_{dh}$) (50 °C – 380 °C) (%) | Dehydroxylation ($L_{dx}$) (380 °C – 550 °C) (%) | Decarbonation($L_{dc}$) (550 °C – 1000 °C) (%) | Bound Water (H) (%) | Calcium Hydroxide (CH) (%) |
|---|---|---|---|---|---|
| M-C | 14.66 | 3.77 | 2.74 | 23.59 | 15.48 |
| M-LS5 | 14.97 | 4.03 | 4.88 | 24.21 | 16.58 |
| M-ES5 | 14.29 | 3.86 | 4.34 | 22.93 | 15.86 |
| M-CES5(400-2) | 14.43 | 4.01 | 5.55 | 23.46 | 16.49 |
| M-CES5(600-2) | 15.15 | 4.30 | 6.27 | 25.13 | 17.68 |
| M-CES15(800-3) | 13.14 | 5.16 | 6.47 | 23.15 | 21.21 |

### *3.5. Microstructural Observations*

Following the TGA analysis, scanning electron microscopy (SEM) was performed on selected representative mixtures to examine the morphology of the hydration products and overall microstructural development. Three mixtures were selected for comparison: the control mixture (M-C), CES5(600-2), and CES15(800-3). These mixtures represent the reference cement system, the comparatively favourable calcination condition within the undecomposed-calcite regime, and the decomposed-calcite regime, respectively. Attention was given to the morphology of the C-S-H-rich matrix, calcium hydroxide (CH)-like crystalline features, and carbonate-related phases. Because the phase assignments are based primarily on morphology in secondary-electron images without complementary chemical or crystallographic analysis, they are considered qualitative.

As shown in Figure 11(a), the control mixture exhibited a relatively continuous C-S-H-rich matrix accompanied by distinct plate-like and needle-like crystalline features. The plate-like features are morphologically consistent with CH, whereas the needle-like features may be associated with AFt-type hydration products. The relatively dense distribution of hydration products provides the reference microstructure against which the CES-containing mixtures can be compared. In calcium carbonate-containing cementitious systems, carbonate-bearing particles may also provide additional surfaces for the nucleation and precipitation of hydration products through heterogeneous nucleation [51,78,79].

A comparatively well-developed hydration-product morphology was observed for CES5(600-2), as shown in Figure 11(b). The microstructure contained an extensive C-S-H-rich matrix with numerous fine fibrous, or needle-like features distributed throughout the hydrated regions, together with plate-like crystalline features. Although the individual phases cannot be definitively identified from secondary-electron morphology alone, the overall appearance suggests a relatively well-developed hydration-product network. This observation is particularly relevant because CES5(600-2) exhibited the highest bound-water content among the investigated undecomposed-calcite CES mixtures, reaching 25.13%, together with a relatively high CH content of 17.68%. The SEM observations therefore provide qualitative microstructural support for the greater hydration development indicated by the TGA analysis. The comparatively favourable microstructure is also consistent with the higher compressive-strength performance of the CES600 condition.

The morphology of CES15(800-3), representing the decomposed-calcite regime, is shown in Figure 11(c). The specimen exhibited a highly heterogeneous but well-developed hydration-product matrix, with numerous fine fibrous/needle-like features and relatively large plate-like crystalline regions. The latter are morphologically consistent with CH-like features. However, interpretation of the CH morphology in this mixture requires particular caution because calcination at 800 °C promotes the decomposition of $CaCO_3$ and formation of CaO, which can subsequently hydrate to form $Ca(OH)_2$. Therefore, the CH observed in the CES15(800-3) specimen may originate from both cement hydration and hydration of CaO initially present in the calcined eggshells. This interpretation is consistent with the substantially higher CH content measured by TGA for this mixture (21.21%) and explains why CH content alone cannot be considered a direct measure of cement hydration in highly calcined CES systems.

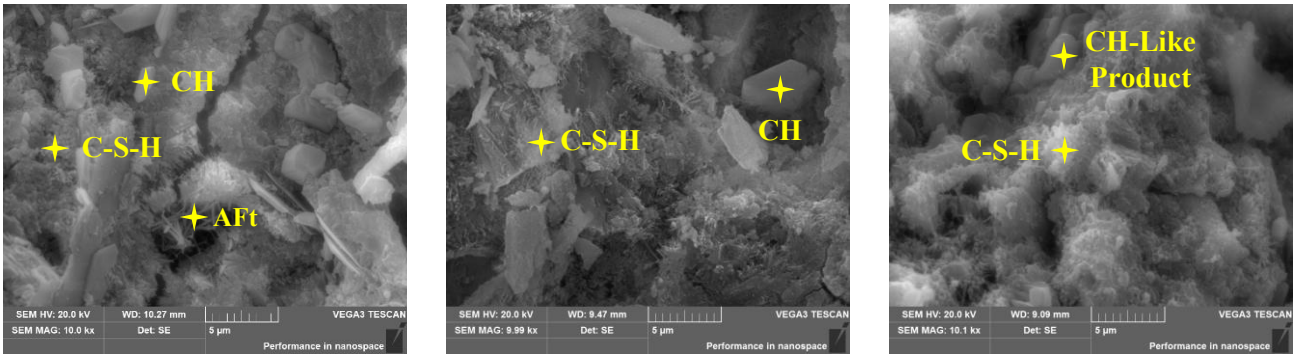


(a) (b) (c)

Figure 11: Microstructural characterization through SEM, (a) Homogenous morphology of control mix, (b) Well-developed heterogenous C-S-H-rich matrix with abundant crystalline feature of CES5(600-2) mortar mix, (c) Highly complex heterogeneous morphology of CES15(800-3) mortar mix.

Carbonate-related crystalline features were also observed in selected CES-containing specimens. Vaterite-like morphologies were observed in highly calcined CES mixtures, as shown below in Figure 12. The presence of vaterite may be associated with the carbonation of calcium-containing hydration products or with the transformation and recrystallization of calcium carbonate phases during hydration and subsequent exposure to atmospheric $CO_2$ [42,66–71]. Similarly, the limited occurrence of calcite-like features may represent residual or unreacted $CaCO_3$ originating from the eggshell powder or carbonate formed through carbonation of the hydrated matrix. Therefore, these features should be regarded as indicative carbonate-related morphologies rather than definitive phase identifications based solely on SEM.

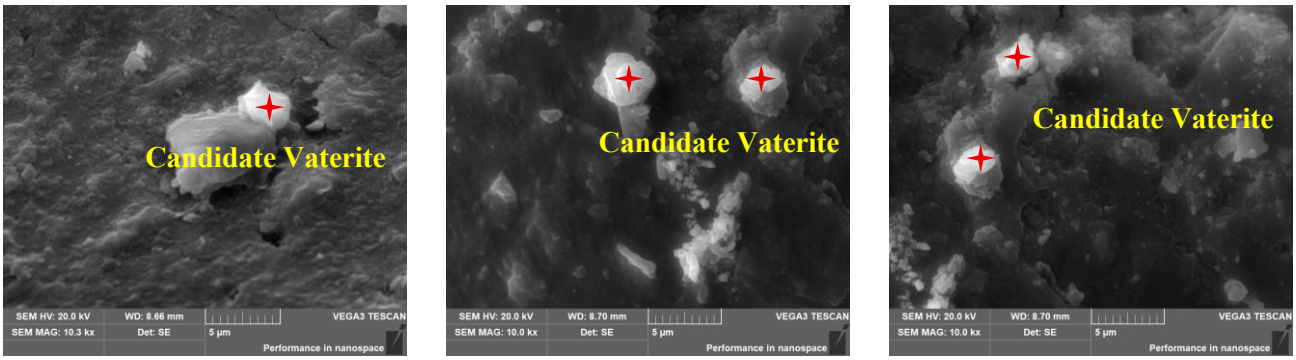


(a) (b) (c)

Figure 12: Some traces of vaterite-like carbonates in CES15(800-3)

Overall, the SEM observations indicate that calcination of eggshells did not fundamentally alter the general morphology of the hydration products, which remained dominated by a C-S-H-rich matrix accompanied by plate-like and fibrous/needle-like crystalline features. Nevertheless, the degree and distribution of hydration products varied with calcination condition. Among the undecomposed-calcite mixtures, CES5(600-2) exhibited a comparatively well-developed hydration morphology, consistent with its highest bound-water content and favourable compressive-strength performance. In contrast, the morphology of CES15(800-3) reflects the more complex chemistry associated with highly calcined eggshells, particularly the contribution of CaO-derived $Ca(OH)_2$. Thus, the SEM results provide qualitative morphological evidence supporting the strength and TGA findings, while phase identification beyond morphological attribution would require complementary techniques such as EDS or XRD.

## 4. Conclusions

This study investigated the influence of the degree of calcination of waste eggshell powder on the fresh behaviour, 28-day compressive strength, hydration characteristics, and microstructural development of cementitious mortar. Eggshells were calcined at 400, 600, and 800 °C for holding durations of 1–3 h, and the resulting powders were evaluated at different cement-replacement levels. The main conclusions are as follows:

- Flow consistency was strongly influenced by the state of the eggshell powder. Limestone generally increased mortar flow, whereas uncalcined eggshell reduced flow relative to the control, which is attributed primarily to the presence of the residual organic membrane. Calcination modified the rheological response of the eggshell powder and removed the limitation associated with the organic matrix; however, the CES mixtures exhibited a non-monotonic response with calcination condition and replacement level.
- The compressive-strength response depended on both replacement level and calcination regime. Mixtures containing predominantly undecomposed calcite generally achieved their highest strength at 5% replacement. In contrast, the response of partially decomposed CES was less systematic because of the more complex phase assemblage containing residual $CaCO_3$ together with dissociated lime. Under the investigated conditions, CES calcined at 800 °C for 3 h with 15% replacement exhibited the highest strength within the partially decomposed regime, whereas CES-600(2) represented the most favourable condition within the calcite-rich regime.
- TGA/DTG analysis demonstrated that calcination condition altered the hydration characteristics of CES-containing systems. The thermal response was associated with dehydration, dehydroxylation, and decarbonation processes corresponding broadly to hydration products, calcium hydroxide, and carbonate phases. Among the calcite-rich mixtures, CES-600(2) exhibited the highest bound-water content (25.13%), exceeding both the control (23.59%) and limestone-based mixturs (24.21%), and this result was consistent with its favourable compressive-strength performance.
- The interpretation of calcium hydroxide content depended strongly on the calcination regime. CES-600(2) exhibited a relatively high CH content (17.68%) together with the highest bound-water content, supporting a comparatively favourable hydration state within the calcite-rich regime. In contrast, CES-800(3) with 15% replacement level exhibited a substantially higher CH content (21.21%), but this value cannot be interpreted solely as evidence of greater cement hydration because CaO generated during calcination can subsequently hydrate to $Ca(OH)_2$.
- SEM observations provided qualitative microstructural support for the mechanical and thermal analyses. The control and CES-containing mixtures exhibited C-S-H-rich matrices accompanied by plate-like and needle-like crystalline features. CES after showed a comparatively well-developed hydration-product morphology consistent with its higher bound-water content and favourable strength, whereas CES-800(3) exhibited a more complex morphology consistent with the altered phase assemblage associated with higher calcination severity. Carbonate-rich, vaterite-like morphologies were also observed in the highly calcined mixture; however, these assignments remain indicative because phase-specific chemical or crystallographic confirmation was not performed.

Overall, the results demonstrate that the degree of calcination is a key parameter governing the performance and hydration behaviour of eggshell powder used as a cement replacement. The transition from predominantly calcite-rich eggshell to partially decomposed material changes the balance between residual $CaCO_3$ and dissociated lime, thereby influencing fresh behaviour, strength development, and hydration characteristics. Within the investigated conditions, CES-600(2) provided the most favourable combination of hydration and mechanical performance in the calcite-rich regime, while the behaviour of the partially decomposed regime was more complex and requires broader investigation to establish a general optimum.

**References**


[1] S. Tsivilis, E. Chaniotakis, E. Badogiannis, G. Pahoulas, A. Ilias, A study on the parameters affecting the properties of Portland limestone cements, Cem. Concr. Compos. 21 (1999) 107–116. https://doi.org/10.1016/S0958-9465(98)00031-6.

[2] V. Bonavetti, H. Donza, G. Menéndez, O. Cabrera, E.F. Irassar, Limestone filler cement in low w/c concrete: A rational use of energy, Cem. Concr. Res. 33 (2003) 865–871. https://doi.org/10.1016/S0008-8846(02)01087-6.

[3] S. Maqsood, H.Y. Ng, M. Afzal, S.U. Rehman, M.F. Ayyub, Global Eggshell Properties: Characterizing Variability for Sustainable Partial Cement Replacement in Hong Kong's Concrete, Preprints (Basel). (2025). https://doi.org/10.20944/preprints202310.1834.v3.

[4] M. Kristl, S. Jurak, M. Brus, V. Sem, J. Kristl, Evaluation of calcium carbonate in eggshells using thermal analysis, J. Therm. Anal. Calorim. 138 (2019) 2751–2758. https://doi.org/10.1007/s10973-019-08678-8.

[5] B.W. Chong, P. Gujar, X. Shi, P. Suraneni, Assessment of waste eggshell powder as a limestone alternative in portland cement, Mater. Struct. 57 (2024) 219. https://doi.org/10.1617/s11527-024-02478-9.

[6] ASTM, C911 - Standard Specification for Quicklime, Hydrated Lime, and Limestone for Selected Chemical and Industrial Uses, Pennsylvania, 2023. https://doi.org/DOI: 10.1520/C0911-19.

[7] T. Matschei, B. Lothenbach, F.P. Glasser, Thermodynamic properties of Portland cement hydrates in the system CaO–Al2O3–SiO2–CaSO4–CaCO3–H2O, 37 (2007) 1379–1410. https://doi.org/10.1016/j.cemconres.2007.06.002.

[8] P. Pliya, D. Cree, Limestone derived eggshell powder as a replacement in Portland cement mortar, Constr. Build. Mater. 95 (2015) 1–9. https://doi.org/10.1016/j.conbuildmat.2015.07.103.

[9] S. Niyasom, N. Tangboriboon, Development of biomaterial fillers using eggshells, water hyacinth fibers, and banana fibers for green concrete construction, Constr. Build. Mater. 283 (2021) 122627. https://doi.org/10.1016/j.conbuildmat.2021.122627.

[10] A. Yerramala, Properties of concrete with eggshell powder as cement replacement, Indian Concrete Journal 88 (2014) 94–102.

[11] D. Gowsika, S. Sarankokila, K. Sargunan, Experimental investigation of egg shell powder as partial replacement with cement in concrete, International Journal of Engineering Trends and Technology 14 (2) (2014) 65–68.

[12] N. Parthasarathi, M. Prakash, K.S. Satyanarayanan, Experimental study on partial replacement of cement with egg shell powder and silica fume, Rasayan Journal of Chemistry 10 (2017) 442–449. https://doi.org/10.7324/RJC.2017.1021689.

[13] A. Sanusi, E.E. Ndububa, A.A. Adeleke, I.I. Obianyo, U.I. Wambai, Y.M. Kudu, I. Mohammed, Physico-mechanical and chemical performance of Portland cement modified with eggshell powder for sustainable construction, 2026. https://doi.org/10.1038/s41598-026-56311-0.

[14] G.C. Ribeiro, G.R.Z. Garcia, S. Ribeiro, Influence of the Addition of Eggshell Ash on the Strength of 1:3 Mortars, Cerâmica 72 (2026) 1–8. https://doi.org/10.1590/oxfe5937.

[15] J. Johnycal, O.C. Lian, M.R.M. Zain, N. Zuhan, N.N. Kencanawati, A. Mishad, Experimental Study on Properties of Cement Mortar Containing Calcined Eggshell Powder at 600 °C and 800 °C, in: W.W.A. Zailani, H. Mansor, M. Usman, A. Adesina (Eds.), Proceedings of the 16th International Conference on Concrete Engineering and Technology, Springer Nature Singapore, Singapore, 2026: pp. 146–158.

[16] A.F. Şenol, Ö. Çalışkan, Effect of eggshell powder calcined at different temperatures on the workability and mechanical properties of cement-based mortars, Ömer Halisdemir Üniversitesi Mühendislik Bilimleri Dergisi 15 (2025) 1–1. https://doi.org/10.28948/ngumuh.1790353.

[17] F. Ujin, K.S. Ali, Z.Y.H. Harith, Viability of Using Eggshells Ash Affecting the Setting Time of Cement, International Journal of Civil, Environmental, Structural, Construction and Architectural Engineering 10 (2016) 327–331.

[18] S. Maqsood, L.S.S. Eddie, Effect of using Calcined Eggshells as a Cementitious Material on Early Performance, Constr. Build. Mater. 318 (2022) 1–15. https://doi.org/10.1016/j.conbuildmat.2021.126170.

[19] H. Binici, O. Aksogan, A.H. Sevinc, E. Cinpolat, Mechanical and radioactivity shielding performances of mortars made with cement, sand and egg shells, Constr. Build. Mater. 93 (2015) 1145–1150. https://doi.org/10.1016/j.conbuildmat.2015.05.020.

[20] A.H. Sevinç, M.Y. Durgun, A novel epoxy-based composite with eggshell, PVC sawdust, wood sawdust and vermiculite: An investigation on radiation absorption and various engineering properties, Constr. Build. Mater. 300 (2021). https://doi.org/10.1016/j.conbuildmat.2021.123985.

[21] E. Tavlı, R. Artan, Utilization of Eggshell Powder in Cement Mortars: Enhancing Mechanical and Thermal Properties for Sustainable Construction, The Open Construction & Building Technology Journal 20 (2026) 1–23. https://doi.org/10.2174/0118748368445575251210172203.

[22] D. Cree, P. Pliya, Effect of elevated temperature on eggshell, eggshell powder and eggshell powder mortars for masonry applications, Journal of Building Engineering 26 (2019) 100852. https://doi.org/10.1016/j.jobe.2019.100852.

[23] N. Shiferaw, L. Habte, T. Thenepalli, J.W. Ahn, Effect of eggshell powder on the hydration of cement paste, Materials 12 (2019). https://doi.org/10.3390/ma12152483.

[24] A.A. Dezfouli, Effect of Eggshell Powder Application on the Early and Hardened Properties of Concrete, Journal of Civil Engineering and Materials Application 4 (2020) 209–221. https://doi.org/10.22034/JCEMA.2020.241853.1036.

[25] M.S. Islam, S.C. Paul, B.J. Mohr, Hydration heat comparison of portland cement blends with commonly available supplementary cementitious materials (SCMs) by isothermal calorimetry, Next Sustainability 7 (2026) 100258. https://doi.org/10.1016/j.nxsust.2026.100258.

[26] R.H. Wang, F.Z. Ren, Z.J. Huang, H. Zhao, H.Y. Guo, J.Y. Cui, Research of jointing impact crushing, flotation and acid treatment of avian eggshell membrane extraction method, Science and Technology of Food Industry 33 (2012) 291–299.

[27] Y.S. Wang, R. Lin, T. Kim, J.Y. Lim, S.J. Kwon, X.Y. Wang, Development and characterization of ternary blended cement incorporating slag and thermally activated waste eggshell: Hydration, microstructure, macro properties, and carbonation durability, Constr. Build. Mater. 490 (2025) 142569. https://doi.org/10.1016/j.conbuildmat.2025.142569.

[28] Y. He, D. Che, X. Ouyang, Y. Niu, Surface Properties of Eggshell Powder and Its Influence on Cement Hydration, Materials 15 (2022). https://doi.org/10.3390/ma15217633.

[29] C.B. Wei, G. Pratik, S. Xijun, S. Prannoy, Valorization of Waste Eggshell as a Limestone Alternative for High-Volume Incorporation into Portland Cement, Journal of Materials in Civil Engineering 38 (2026) 4025617. https://doi.org/10.1061/JMCEE7.MTENG-21776.

[30] S. Yoo, J.S. Hsieh, P. Zou, J. Kokoszka, Utilization of calcium carbonate particles from eggshell waste as coating pigments for ink-jet printing paper, Bioresour. Technol. 100 (2009) 6416–6421. https://doi.org/10.1016/j.biortech.2009.06.112.

[31] D. Cree, A. Rutter, Sustainable Bio-Inspired Limestone Eggshell Powder for Potential Industrialized Applications, ACS Sustain. Chem. Eng. 3 (2015) 941–949. https://doi.org/10.1021/acssuschemeng.5b00035.

[32] B.H. Ngayakamo, Transforming cement mortar performance: impact of eggshell powder as an eco-friendly cement substitute, Discover Concrete and Cement 1 (2025) 1–14. https://doi.org/10.1007/s44416-025-00021-9.

[33] Z. Li, Materials for Making Concrete, in: Advanced Concrete Technology, 2011th ed., John Wiley and Sons, New Jersey, 2011: pp. 23–93.

[34] J. Beaudoin, I. Odler, Hydration, Setting and Hardening of Portland Cement, in: Lea's Chemistry of Cement and Concrete, 5th ed., Elsevier Ltd., 2019: pp. 157–250. https://doi.org/10.1016/B978-0-08-100773-0.00005-8.

[35] H.F.W. Taylor, Hydration of the calcium silicate phases, in: Cement Chemistry, 2nd ed., Thomas Telford Publishing, London, 1997: pp. 113–156.

[36] H.F.W. Taylor, Hydration of Portland Cement, in: Cement Chemistry, 2nd ed., Thomas Telford, London, 1997: pp. 187–225.

[37] K. De Weerdt, M. Ben Haha, G. Le Saout, K.O. Kjellsen, H. Justnes, B. Lothenbach, Hydration mechanisms of ternary Portland cements containing limestone powder and fly ash, Cem. Concr. Res. 41 (2011) 279–291. https://doi.org/10.1016/j.cemconres.2010.11.014.

[38] F. Deschner, F. Winnefeld, B. Lothenbach, S. Seufert, P. Schwesig, S. Dittrich, F. Goetz-neunhoeffer, J. Neubauer, Hydration of Portland cement with high replacement by siliceous fly ash, Cem. Concr. Res. 42 (2012) 1389–1400. https://doi.org/10.1016/j.cemconres.2012.06.009.

[39] S.J. Kim, K.H. Yang, G.D. Moon, Hydration characteristics of low-heat cement substituted by fly ash and limestone powder, Materials 8 (2015) 5847–5861. https://doi.org/10.3390/ma8095277.

[40] F.U.A. Shaikh, S.W.M. Supit, S. Barbhuiya, Microstructure and Nanoscaled Characterization of HVFA Cement Paste Containing Nano-SiO2 and Nano-CaCO3, Journal of Materials in Civil Engineering 29 (2017) 04017063. https://doi.org/10.1061/(asce)mt.1943-5533.0001898.

[41] N. Saadatkhah, A. Carillo Garcia, S. Ackermann, P. Leclerc, M. Latifi, S. Samih, G.S. Patience, J. Chaouki, Experimental Methods in Chemical Engineering: Thermogravimetric Analysis—TGA, Can. J. Chem. Eng. 98 (2020) 34–43. https://doi.org/10.1002/cjce.23673.

[42] M. Aqel, D.K. Panesar, Hydration kinetics and compressive strength of steam-cured cement pastes and mortars containing limestone filler, Constr. Build. Mater. 113 (2016) 359–368. https://doi.org/10.1016/j.conbuildmat.2016.03.031.

[43] M. Cyr, P. Lawrence, E. Ringot, Efficiency of mineral admixtures in mortars: Quantification of the physical and chemical effects of fine admixtures in relation with compressive strength, Cem. Concr. Res. 36 (2006) 264–277. https://doi.org/10.1016/j.cemconres.2005.07.001.

[44] I. Soroka, N. Stern, Calcareous fillers and the compressive strength of portland cement, Cement and Cocnrete Research 6 (1975) 367–376. https://doi.org/10.1016/0008-8846(76)90099-5.

[45] E.F. Irassar, Sulfate attack on cementitious materials containing limestone filler - A review, Cem. Concr. Res. 39 (2009) 241–254. https://doi.org/10.1016/j.cemconres.2008.11.007.

[46] S. Rode, N. Oyabu, K. Kobayashi, H. Yamada, A. Kühnle, True atomic-resolution imaging of (1014) calcite in aqueous solution by frequency modulation atomic force microscopy, Langmuir 25 (2009) 2850–2853. https://doi.org/10.1021/la803448v.

[47] K. Vance, M. Aguayo, T. Oey, G. Sant, N. Neithalath, Hydration and strength development in ternary portland cement blends containing limestone and fly ash or metakaolin, Cem. Concr. Compos. 39 (2013) 93–103. https://doi.org/10.1016/j.cemconcomp.2013.03.028.

[48] D.P. Bentz, A. Ardani, T. Barrett, S.Z. Jones, D. Lootens, M.A. Peltz, T. Sato, P.E. Stutzman, J. Tanesi, W.J. Weiss, Multi-scale investigation of the performance of limestone in concrete, Constr. Build. Mater. 75 (2015) 1–10. https://doi.org/10.1016/j.conbuildmat.2014.10.042.

[49] P. Thongsanitgarn, W. Wongkeo, A. Chaipanich, C.S. Poon, Heat of hydration of Portland high-calcium fly ash cement incorporating limestone powder: Effect of limestone particle size, Constr. Build. Mater. 66 (2014) 410–417. https://doi.org/10.1016/j.conbuildmat.2014.05.060.

[50] D. Wang, C. Shi, N. Farzadnia, Z. Shi, H. Jia, A review on effects of limestone powder on the properties of concrete, Constr. Build. Mater. 192 (2018) 153–166. https://doi.org/10.1016/j.conbuildmat.2018.10.119.

[51] N. Shiferaw, L. Habte, T. Thenepalli, J.W. Ahn, Effect of eggshell powder on the hydration of cement paste, Materials 12 (2019). https://doi.org/10.3390/ma12152483.

[52] BSI, Methods of testing Composition, Specifications and Conformity Criteria for Common Cements, in: BS EN 197-1, 2011: p. 50.

[53] British Standards Institution, BS EN 196-1:2016 – Methods of testing cement. Determination of strength, London, United Kingdom, 2016. https://doi.org/https://doi.org/10.3403/30291447U.

[54] T.N. Blanton, C.L. Barnes, Quantitative Analysis of Calcium Oxide Desiccant Conversion to Calcium Hydroxide Using X-ray Diffraction, Powder Diffr. 19 (2004) 201–201. https://doi.org/10.1154/1.1779815.

[55] N. Tangboriboon, R. Kunanuruksapong, A. Sirivat, R. Kunanuruksapong, A. Sirivat, Preparation and properties of calcium oxide from eggshells via calcination, Materials Science- Poland 30 (2012) 313–322. https://doi.org/10.2478/s13536-012-0055-7.

[56] A. Lesbani, P. Tamba, R. Mohadi, Fahmariyanti, Preparation of calcium oxide from Achatina fulica as catalyst for production of biodiesel from waste cooking oil, Indonesian Journal of Chemistry 13 (2013) 176–180. https://doi.org/10.22146/ijc.21302.

[57] D. Han, J.Y. Yoon, J.H. Kim, Control of Viscosity of Cementitious Materials Using Waste Limestone Powder, Int. J. Concr. Struct. Mater. 13 (2019) 28. https://doi.org/10.1186/s40069-018-0325-9.

[58] J. Zhang, Z. Li, Impact of the Limestone Powder on the Properties of Cement Paste and Mortar, Applied Mechanics and Materials 174–177 (2012) 236–240. https://doi.org/10.4028/www.scientific.net/AMM.174-177.236.

[59] S. Zhang, Y. Zhao, Z. Zhang, T. Xiang, M. Guo, D. Chen, Unraveling the regulatory mechanism of limestone powder particle size and replacement level on rheology of cement paste, Powder Technol. 475 (2026) 122323. https://doi.org/10.1016/j.powtec.2026.122323.

[60] A. Yahia, M. Tanimura, Y. Shimoyama, Rheological properties of highly flowable mortar containing limestone filler-effect of powder content and W/C ratio, Cem. Concr. Res. 35 (2005) 532–539. https://doi.org/10.1016/j.cemconres.2004.05.008.

[61] G. De Schutter, Effect of limestone filler as mineral addition in self compacting concrete, in: 36th Conference on Our World in Concrete and Structures: "Recenet Advances in the Technology of Fresh Concrete," Ghent University, Department of Structural Engineering, Ghent, 2011: pp. 49–54. https://biblio.ugent.be/publication/2939937.

[62] E.J. Sellevold, D.H. Bager, E.K. Jensen, T. Knudsen, Silica fume-cement pastes: hydration and pore structure, in: Condensed Silica Fume in Concrete, Institutt for Bygningsmateriallære, Norges Tekniske Høgskole, Norway, 1982.

[63] V.S. Ramachandran, Z. Chun-Mei, Thermal analysis of the 3CaO· Al2O3-CaSO4· 2H2O-CaCO3-H2O system, Thermochim. Acta 106 (1986) 273–282.

[64] E.F. Irassar, D. Violini, V.F. Rahhal, C. Milanesi, M.A. Trezza, V.L. Bonavetti, Influence of limestone content, gypsum content and fineness on early age properties of Portland limestone cement produced by inter-grinding, Cem. Concr. Compos. 33 (2011) 192–200. https://doi.org/10.1016/j.cemconcomp.2010.10.001.

[65] A. Ipavec, R. Gabrovšek, T. Vuk, V. Kaučič, J. MačEk, A. Meden, Carboaluminate phases formation during the hydration of calcite-containing Portland cement, Journal of the American Ceramic Society 94 (2011) 1238–1242. https://doi.org/10.1111/j.1551-2916.2010.04201.x.

[66] J.M. Stepkowska, E.T., Pérez-Rodríguez, J.L., Sayagues, M.J. Martinez-Blanes, Calcite, vaterite and aragonite forming on cement hydration from liquid and gaseous phase, J. Therm. Anal. Calorim. 73 (2003) 247–269.

[67] A. Hidalgo, C. Domingo, C. Garcia, S. Petit, C. Andrade, C. Alonso, Microstructural changes induced in Portland cement-based materials due to natural and supercritical carbonation, J. Mater. Sci. 43 (2008) 3101–3111. https://doi.org/10.1007/s10853-008-2521-5.

[68] A. Morandeau, M. Thiéry, P. Dangla, Investigation of the carbonation mechanism of CH and C-S-H in terms of kinetics, microstructure changes and moisture properties, Cem. Concr. Res. 56 (2014) 153–170. https://doi.org/10.1016/j.cemconres.2013.11.015.

[69] Y. Fang, J. Chang, Microstructure changes of waste hydrated cement paste induced by accelerated carbonation, Constr. Build. Mater. 76 (2015) 360–365. https://doi.org/10.1016/j.conbuildmat.2014.12.017.

[70] W. Ashraf, Carbonation of cement-based materials: Challenges and opportunities, Constr. Build. Mater. 120 (2016) 558–570. https://doi.org/10.1016/j.conbuildmat.2016.05.080.

[71] A. Trník, L. Scheinherrová, T. Kulovaná, R. Černý, Simultaneous Differential Scanning Calorimetry and Thermogravimetric Analysis of Portland Cement as a Function of Age, Int. J. Thermophys. 37 (2016) 1–9. https://doi.org/10.1007/s10765-015-2028-7.

[72] G.M. Azarov, E. V. Maiorova, M.A. Oborina, A. V. Belyakov, Wollastonite raw materials and their applications (a review), Glass and Ceramics 52 (1995) 237–240. https://doi.org/10.1007/BF00681090.

[73] N.I. Demidenko, L.I. Podzorova, V.S. Rozanova, V.A. Skorokhodov, V.Y. Shevchenko, Wollastonite as a new kind of natural material (a review), Glass and Ceramics (English Translation of Steklo i Keramika) 58 (2001) 308–311. https://doi.org/10.1023/A:1013931009149.

[74] L.D. Maxim, E.E. McConnell, A review of the toxicology and epidemiology of wollastonite, Inhal. Toxicol. 17 (2005) 451–466. https://doi.org/10.1080/08958370591002030.

[75] R.I. Khan, W. Ashraf, Effects of ground wollastonite on cement hydration kinetics and strength development, Constr. Build. Mater. 218 (2019) 150–161. https://doi.org/10.1016/j.conbuildmat.2019.05.061.

[76] Z. He, A. Shen, Z. Lyu, Y. Li, H. Wu, W. Wang, Effect of wollastonite microfibers as cement replacement on the properties of cementitious composites: A review, Constr. Build. Mater. 261 (2020) 119920. https://doi.org/10.1016/j.conbuildmat.2020.119920.

[77] N.A. Nair, V. Sairam, Research initiatives on the influence of wollastonite in cement-based construction material- A review, J. Clean. Prod. 283 (2021) 124665. https://doi.org/10.1016/j.jclepro.2020.124665.

[78] P. Lawrence, M. Cyr, E. Ringot, Mineral admixtures in mortars: Effect of inert materials on short-term hydration, Cem. Concr. Res. 33 (2003) 1939–1947. https://doi.org/10.1016/S0008-8846(03)00183-2.

[79] E.H. Kadri, S. Aggoun, G. De Schutter, K. Ezziane, Combined effect of chemical nature and fineness of mineral powders on Portland cement hydration, Materials and Structures/Materiaux et Constructions 43 (2010) 665–673. https://doi.org/10.1617/s11527-009-9519-6.